A CLIMATOLOGY OF STRATOCUMULUS CLOUD PROPERTIES IN THE PACS REGION

C. W. Fairall, Duane Hazen, Brad Orr, Dana Lane, J. E. Hare, M. Ryan, and A. S. Frisch
June 20, 2001

INTRODUCTION

The representation of clouds and their interactions with the Earth's radiation field are a major source of uncertainty in efforts to predict climate change through General Circulation Models (GCMs). Radiative surface cooling associated with subtropical stratocumulus clouds and turbulent interfacial fluxes associated with stratocumulus boundary-layer dynamics are primary factors in producing the observed sea surface temperature structure of the Eastern Pacific. NOAA has recently initiated a program of study called EPIC that includes investigations of clouds in the PACS region. The EPIC observational strategy involves a combination of limited and comprehensive process studies, coupled with other oceanographic and meteorological studies of the equatorial region. Since 1999 ETL has been conducting a three-year study of clouds, surface fluxes, and boundary layer properties in the Eastern Pacific as part of the EPIC monitoring program.

PROJECT GOALS

In this project we implemented a modest ship-based cloud measurement program to obtain statistics on key surface, MBL, and low-cloud macrophysical, microphysical, and radiative properties. Obviously, we cannot completely elucidate such a spectrum of complicated processes with our modest monitoring effort. Rather, our goal is to acquire a good sample of most of the relevant bulk variables that are commonly used in GCM parameterizations dealing with these problems. These will then be compared to known relationships in other well-studied regimes. While not comprehensive, this data will still be useful for MBL/cloud modelers (both statistically and for specific simulations) and to improve satellite retrieval methods for deducing MBL and cloud properties on larger spatial and temporal scales.

To summarize, our objectives are to

*Obtain new measurements of surface, cloud, and MBL statistics for simple comparison to existing data on northern hemisphere stratocumulus systems.

*Obtain quantitative information on cloud droplet sizes plus properties and probability of occurrence of drizzle and possible links to deviations from adiabatic values for W.

*Examine applicability of existing bulk parameterizations of stratocumulus radiative properties for the Peruvian/Equatorial regime.

*Obtain basic data characterization of surface cloud forcing and possible ocean-atmosphere

coupling through stratocumulus-SST interactions.

*Provide periodic, higher quality, more accurate near-surface data for intercomparison with ship-based IMET and buoy-based meteorological measurements.

*Provide high quality measurements of basic surface, MBL and cloud parameters for 'calibration' of satellite retrieval techniques.

METHODOLOGY

We are conducting an enhanced monitoring cloud and MBL measurement program to supplement the measurements made on the NOAA ships (*R/V's Ka'imi Moana* and *Ronald H. Brown*) servicing the TAO buoys in the PACS region. The field program is built around regularly scheduled service visits to the 95 W and the 110 W buoy lines. The 95W line is in the main stratocumulus belt and the 110W line as at the western edge. An instrument package has been developed that can be installed on either ship. The instruments (see Table 1) consist of a cloud ceilometer, an S-band cloud/precipitation Doppler radar, a water vapor/liquid microwave radiometer (MWR), and an automated air-sea flux package including a sonic anemometer, a pair of pyranometers, a pair of pyrgeometers, slow air temperature and humidity sensors, and a ship-motion package for direct turbulent flux corrections.

This set of instruments will allow computation of low cloud statistics (integrated liquid water content, cloud base height, and fraction) and the complete surface energy budget of the oceanic and atmospheric boundary layers. The cloud statistics by themselves will be of interest to cloud modelers and for improving satellite retrieval methods. When combined with measurements of downward longwave and shortwave radiative fluxes, they will allow computation of cloud IR and visible optical thicknesses plus the surface cloud radiative forcing, a key diagnostic variable in climate models. For the fall cruises we archived data from the *Ronald H. Brown* scanning C-band Doppler radar. This gives a information on the spatial structure of precipitating systems. We believe it is sensitive enough to detect stratocumulus clouds within 50 km of the ship. We also deployed the ETL K-band mm-wave cloud radar package on one cruise (Fall 2000) in the 3-year monitoring study. Specifically, we have made measurements intended to yield the following information:

*Cloud macrophysical statistics: cloud fraction, base height, top height, physical thickness

*Radiative statistics: cloud transmission coefficient, cloud optical thickness, surface cloud radiative forcing (solar and IR)

*MBL statistics: surface fluxes (turbulent, radiative), inversion height, mixed-layer properties

*Simple MBL, cloud/radiative parameterizations: integrated liquid water path (W) vs the theoretical adiabatic value for a well mixed MBL ($W_{adiabat}$), cloud optical thickness vs f, W, cloud transmission coefficient and inferred albedo

*Cloud effective radius vs W

Details on the instruments to be used are given in Table 1; items 9-11 were deployed only in Fall 2000 and will be deployed again in Fall 2001.

Table 1. Instruments and measurements deployed by ETL for the ship-based cloud/MBL monitoring project.

Item	System	Measurement
1	Motion/navigation package	Motion correction for turbulence
2	Sonic anemometer/thermometer	Direct covariance turbulent fluxes
3	Mean SST, air temperature/RH	Bulk turbulent fluxes
4	Pyranometer	Downward solar radiative flux
5	Pyrgeometer	Downward IR radiative flux
6	Ceilometer	Cloud-base height
7	0.92 or 3 GHz Doppler radar profiler	Cloud-top height, MBL microturbulence
8	Rawinsonde	MBL wind, temperature, humidity prof.
9	35 GHz Doppler cloud radar	Cloud microphysical properties
10	20, 31, 90 GHz μwave radiometer	Integrated cloud liquid water
11	Upward pointed IR thermometer	Cloud-base radiative temperature
12	Ronald H. Brown C-band radar	Precipitation spatial structure

RESULTS AND ACCOMPLISHMENTS

**Measurement and Archiving Tasks*

We have completed four mission: fall of 1999 and 2000 and spring of 2000 and 2001. Each mission has included transects of the 95 and 110 buoy lines between 8 S and 12 N. A description of the project, which also includes a preliminary analysis of the fall 99 cruise, is available on the ETL website

http://www7.etl.noaa.gov/programs/PACS/ .

Our major effort so far has been in executing the cruises twice a year and processing the various sets of data into reasonably usable form. We have been collaborating with Nick Bond at PMEL and Leslie Hartten at AL on the atmospheric boundary layer aspects, particularly the transitions associated with cold tongue. Our processing goal is to create as database usable for us, our collaborators, and other EPIC investigators. We are presently archiving data at an ftp site

ftp://ftp.etl.noaa.gov/et7/users/cfairall/EPIC/epicmonitor/

for public use. There are individual directories for the fall99, sp00, fall00, and sp01 cruises. Present status of processed data is given in the following table:

Table 2. Present processed data availability at the ETL PACS ftp sites: D - data available on this site, I - image files only, X - available but not posted.

Mission	Fluxes	Radar profiler	Ceilom.	MWR	Sondes	Cloud radar	C-band radar
fall99	D	I	D	D	D	NA	X*
sp00	D	X	D	D	D	NA	NA
fall00	D	X	D	D	D	I*	I*
sp01	D	X	D	D	X	NA	NA

*see http://www6.etl.noaa.gov/data/pacs/ Contact Michelle Ryan (Michelle.Ryan@noaa.gov); these data are too voluminous to provide over ftp.

The fluxes, ceilometer, and MWR are provided at 10-min and 1-hr time resolution. The cloud radar and radar profiler have 1-hr file structures. The C-band radar has a scan-based file structure.

**Preliminary Data Analysis*

Basic processing of the four missions is nearing completion and we have begun the process of looking at all four data sets together. A 'climatology/monitoring' project implies multiple measurements in the same region to evaluate variability. In this region, the long term variability is dominated by El Nino/La Nina cycles; there is a significant seasonal difference between our Northern Hemisphere spring (NHS) and fall (NHF) cruises. There is also some difference between the 110 W and 95 W transects. Finally, there is short term variability associated with the Madden-Julian oscillation, easterly wave activities, and the Tropical Instability Waves (TIW) in the ocean that cause latitudinal displacements of the sea surface temperature fronts. An example of the SST structure obtained from the NASA TRMM TMI sensor for the Fall 1999 *Brown* transect at 110 W is shown in Fig. 1 (courtesy of Dudley Chelton, OSU). In the remainder of this section we will show various quantities of interest computed as one-day

averages as a function of latitude. One-day averages are shown as a convenience that removes the diurnal cycle and simplifies the display. Here we will show each transect individually to illustrate the variability. In all of the graphs the following symbols are used: circle - fall99; x - spring00; diamond - fall00; star - spring01.

We begin with simple plots of the latitudinal distribution of SST (Fig. 2). Note the seasonal cycle is strongest (about 6 C) at the equator southward and becomes negligible at about 10 N. The odd-looking drop in SST at 10 N and 12 N for the fall99 cruise is associated with a cold pool caused by strong gap winds channeled through the mountains (see Fig. 1). The strong seasonal variation in SST is not mirrored in the sea-air temperature difference (Fig. 3), which is an indication of the boundary layer adjustment processes. There is a minimum in Ts-Ta (about 0.4 C) at or just south of the equator; except for brief spikes caused by deep convective events, the maximum in Ts-Ta (about 2.0 C) occurs at the SST front around 2-3 N. Wind speed is a maximum (about 7 m/s) at the southern end of the transect (Fig. 4a) with a tendency for the NHS winds to be stronger. Note the large variability in near-surface wind speeds north of the equator. Fig. 4b shows the variability of the wind components: strong southeasterlies in the south with a minimum in the E-W component just north of the equator and a tendency for a strengthening of the N-S component approaching the ITCZ in NHF. The boundary layer moisture (Fig. 5a) pattern is closely coupled to SST, however total column water vapor (Fig. 5b) actually shows a much stronger seasonal variation (i.e., a factor of 2 versus just 30% for MBL moisture). Thus, the upper air is much drier south of about 2 N during the NHF. This has important implications for cloud top IR radiative cooling.

Variability of surface heat fluxes (sensible, latent, and net radiation) is shown in Fig. 6. The turbulent fluxes have minima at or just south of the equator. The smaller values of net radiation are, of course, associated with cloudiness. Most of the small values south of the equator occur in the NHS while most of those north of the equator occur during NHF. The cloud fraction (Fig. 7) data shows the large cloud masses in NHF associated with the most active phase of the ITCZ. There is a lot of variability near 8 S which is believed to be associated with variations in the edge of the Peruvian stratocumulus region. Low-cloud base heights (Fig. 8) show values around 600 m, which are very typical for the tropics. Note, however, the cluster of much lower values (less than 400 m) near the equator. These are the equatorial stratocumulus clouds caused by flow of a warm south-equatorial air over the cold tongue. The effect of clouds on the net radiation can be further broken down into solar radiative cloud transmission coefficient (Fig. 9) and solar and IR cloud forcing (Fig. 10). The transmission coefficient removes the variability of the solar intensity. Note the equatorial stratocumulus clouds have rather high transmission coefficients (about 0.85) compared to those at the southern end of the transect (0.5 - 0.9). Typical subtropical stratocumulus (e.g., off California) have transmission coefficients around 0.5.

Cloud forcing is the difference in the observed mean radiative flux versus what the flux would be in the absence of clouds

$$XCF = < R_x > - < R_{x0} > \quad \textbf{(1)}$$

where X=S for solar or L for longwave (IR) and the subscript 0 refers to the clear sky flux. A related variable that is often used is the *maximum* cloud forcing, which is the conditional change in the flux when a cloud is actually present. CF averages clear and cloudy periods but MCF is the difference between overcast (cloud fraction f = 1.0) and clear (cloud fraction f = 0) conditions.

$$MCF = < R_{x1} > - < R_{x0} > \approx f * CF \quad \textbf{(2)}$$

MCF is related to the radiative properties of individual clouds and can, in principle, be directly computed from microphysical/radiative variables while CF is strongly dependent on whether it is cloudy or not. In Fig. 10 we can see that SCF is much more significant than LCF, which is typical for the tropics where low level atmospheric moisture is large. However, the LCF here is quite a bit larger that in the tropical western Pacific. Large excursions of CF are associated with greater cloudiness. We have illustrated the dependence of MCF by plotting CF as a function of cloud fraction (Fig. 11). The correlation of LCF is very good, implying a value for MLCF = 60 W/m^2. The correlation for SCF is not as good, primarily because of the sampling problem of using vertically pointing cloud sensors (i.e., a cloud can be overhead but the sun is at some angle that isn't blocked by the cloud, etc) and the diurnal nature of solar flux although some variability is also caused by differences in cloud thickness and microphysics. The line on the figure corresponds to MSCF=180 W/m^2. This is a fairly strong cloud effect implying that when clouds are present they block, on average, about 60% of the solar flux.

**Cloud Radar Data Example*

In the fall of 2000 the ETL 35 GHz cloud radar was operated successfully for the entire mission. In Fig. 12a we show stratocumulus cloud at about 8 S 95 W; in Fig. 12b we show stratocumulus cloud at about 0 N 95 W. The first cloud deck is associated with normal subtropical stratocumulus from the Peruvian region. These clouds are about 200-300 m thick; the streamer like structures below the clouds are drizzle droplets. Drizzle masks the appearance of cloud base but we know it from the ceilometer. The equatorial clouds are thinner (100-200 m thick) and have no drizzle. It is not clear why the equatorial clouds have no drizzle. It may be due to lower liquid water content or higher levels of cloud condensation nuclei. We are presently working on improving the retrievals of liquid water from the microwave radiometer and the cloud radar.

FUTURE WORK

We are finishing up the climatological analysis of near-surface and simple cloud properties as described above. Our next major analysis task is linking cloud microphysical and radiative properties. To date, these efforts have been hampered by poor column integrated liquid water content retrievals from the MWR. We have spent a lot of time investigating this problem which is due to the reduced sensitivity to cloud liquid water of the MWR in the warm tropics and some uncertainties in the water vapor and liquid water absorption coefficients. We are presently working on 'combined retrieval' methods and expect better cloud LWC values in a few months.

This group has combined with the lidar group at ETL and Ken Gage at the NOAA Aeronomy Laboratory to participate in the EPIC2001 intensive field program this fall. EPIC2001 is a particular set of closely related process studies planned for a 6 week period between 5 September and 25 October of 2001 under the aegis of the overall EPIC program. These studies are focused on the dynamics of the cross-equatorial Hadley circulation along 95W, during the period in which it is strongest, and on associated processes which govern the SST and upper ocean structure. The National Science Foundation (NSF) and NOAA/PACS are cooperating in the funding of this project. This study is partitioned into 'bundles'', each dealing with a particular aspect of the problem. The four bundles respectively address (1) the east Pacific ITCZ, (2) the cross-equatorial ITCZ inflow, (3) ocean processes, particularly in the east Pacific warm pool, and (4) the southern hemisphere stratus region. The scientific background for this project is given in the EPIC plan and in the EPIC2001 Overview and Implementation Plan (Raymond, D., S. Esbensen, M. Gregg, and N. Shay, 1999: EPIC2001: Overview and implementation plan. See ftp://kestrel.nmt.edu/pub/raymond/epic2001/overview.pdf). Following the EPIC2001 field program, ETL will complete a 5th monitoring mission through the TAO array when the *Brown* does the maintenance cruise. The cloud radar will be operated for this cruise.

CONTACTS

Principal Investigators:
C. W. Fairall
cfairall@etl.noaa.gov
phone: 303-497-3253
fax: 303-497-6101

A. S. Frisch
afrisch@etl.noaa.gov
phone: 303-497-6201
fax: 303-497-6181

LINKS

Background on ETL group: http://www7.etl.noaa.gov/air-sea-ice/index.html

ETL PACS/EPIC data site: ftp://ftp.etl.noaa.gov/pub/et7/users/cwf/EPIC/epicmonitor
ETL Radar group PACS site: http://www6.etl.noaa.gov/projects/pacs.html

PACS Site: http://tao.atmos.washington.edu/PACS/
EPIC Science Plan: http://www.atmos.washington.edu/gcg/EPIC/
EPIC2001 Science Plan: ftp://kestrel.nmt.edu/pub/raymond/epic2001/overview.pdf

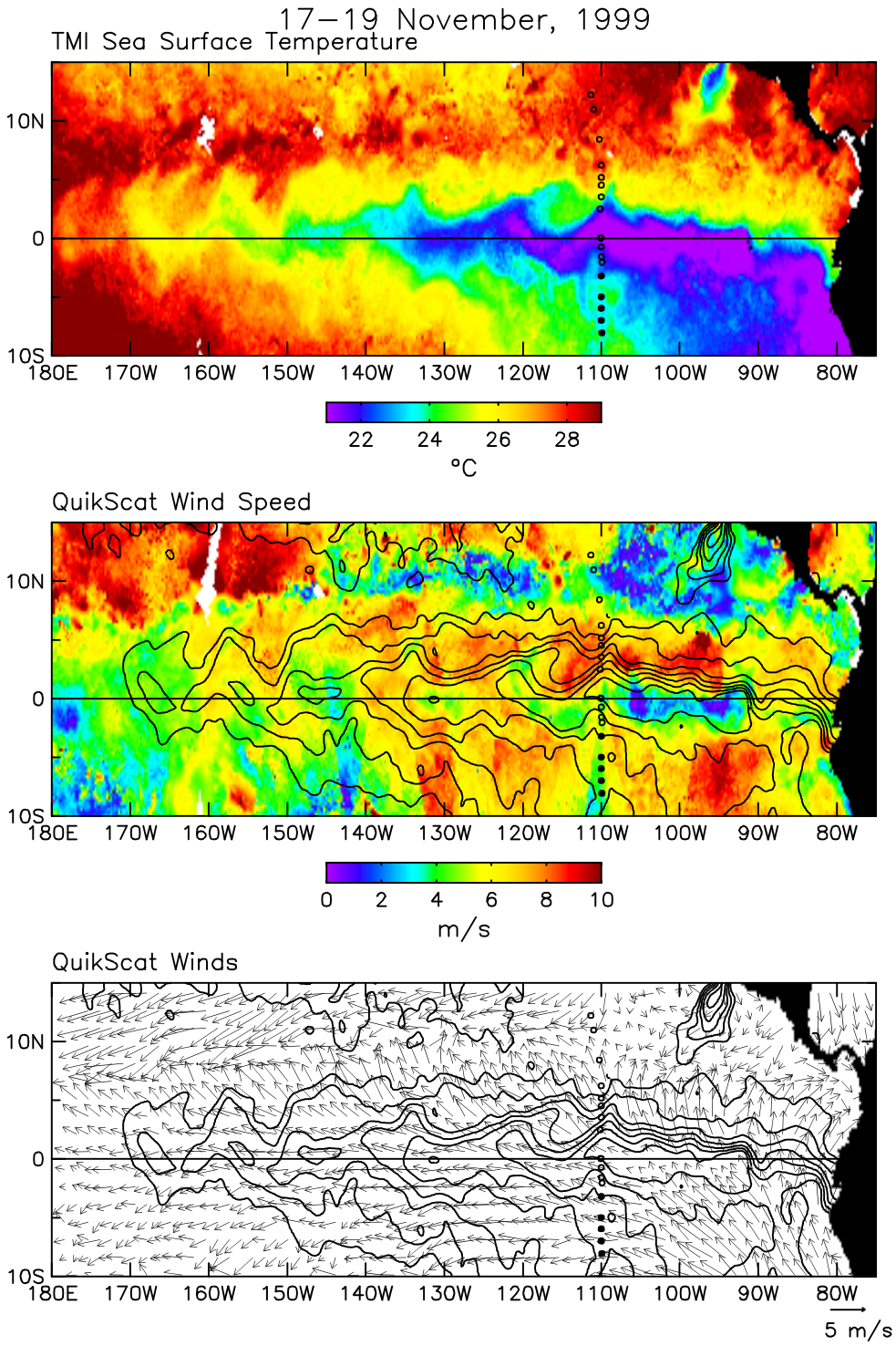

Figure 1. TRMM satellite retrievals of TMI SST (upper panel), QuikScat surface winds with SST contours (middle panel), and QuikScat wind vectors (bottom panel) for the period 17-19 November, 1999 when the *Ronald H. Brown* was making the transit from 12 N to 8 S along 110W.

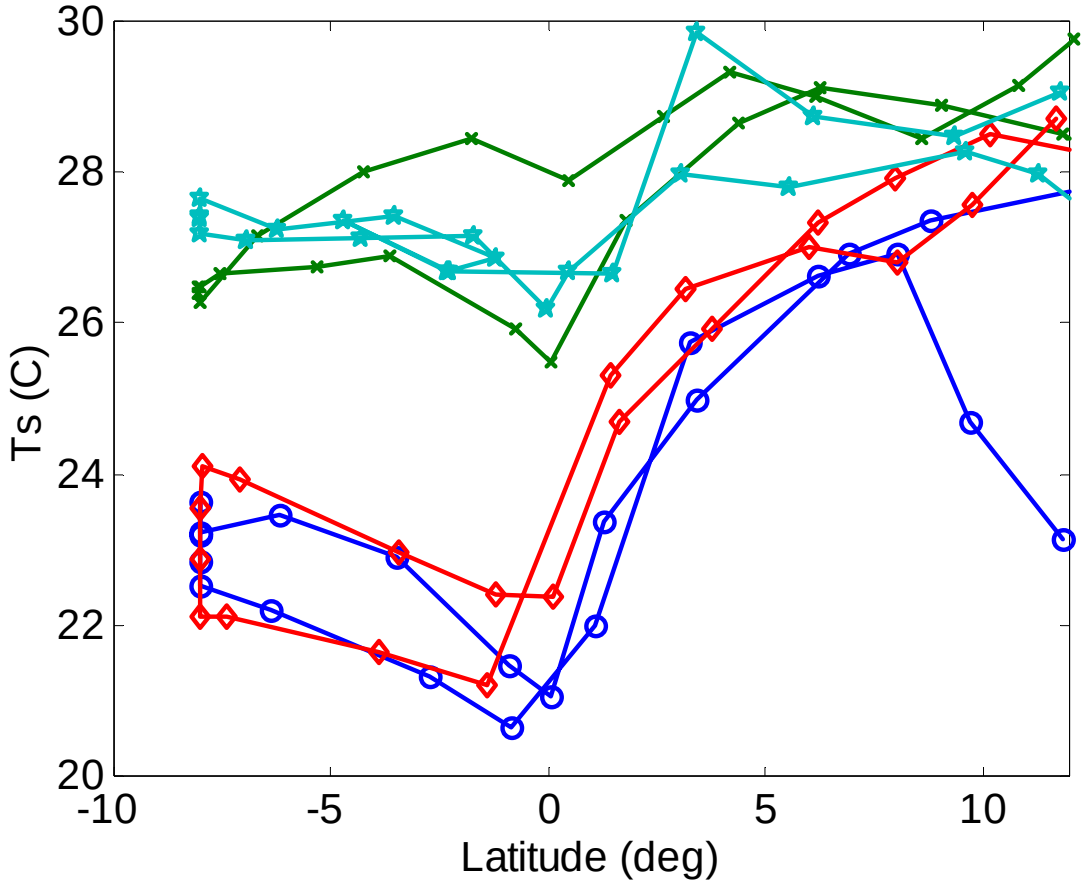

Figure 2. SST versus latitude (daily average values) for the four missions (Fall99 - Spring 01). Symbols are as follows: circle - fall99; x - spring00; diamond - fall00; star - spring01.

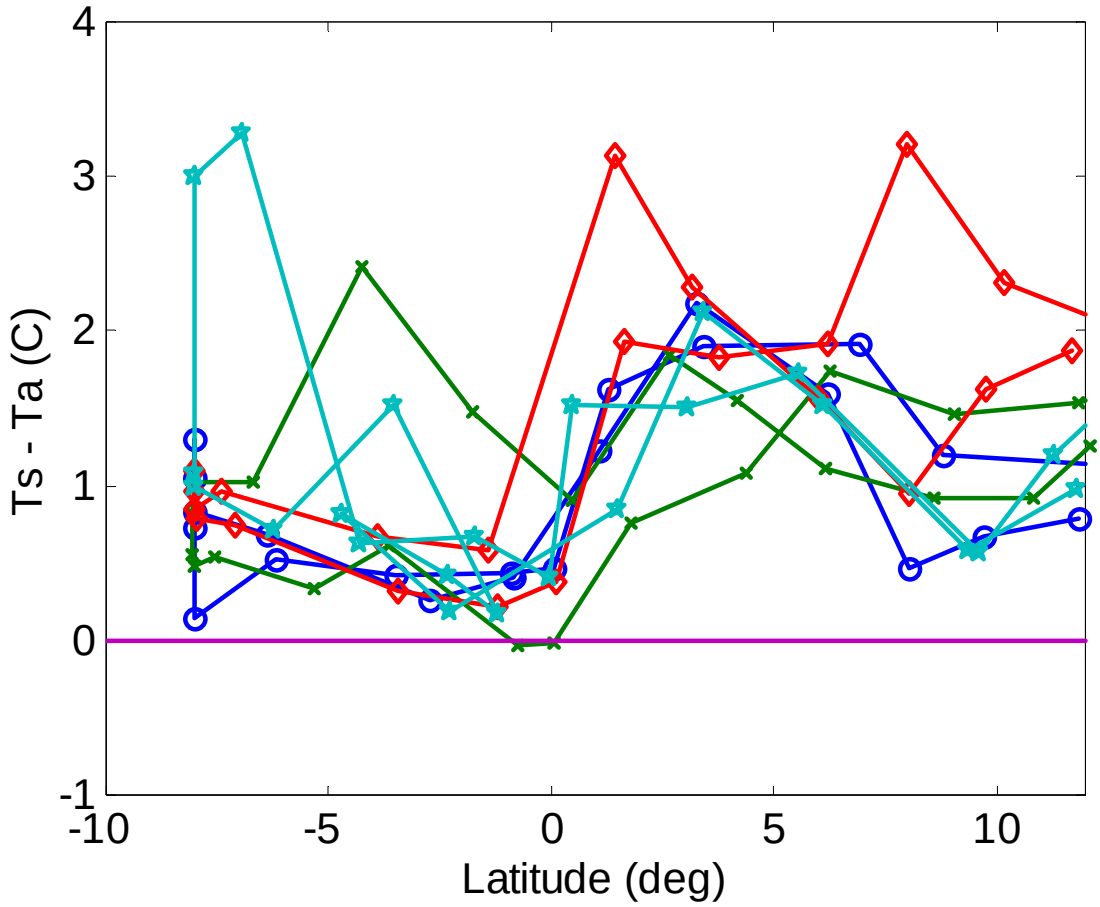

Figure 3. Sea-air temperature difference (SST-Ta) versus latitude (daily average values) for the four missions (Fall99 - Spring 01). Symbols are as follows: circle - fall99; x - spring00; diamond - fall00; star - spring01.

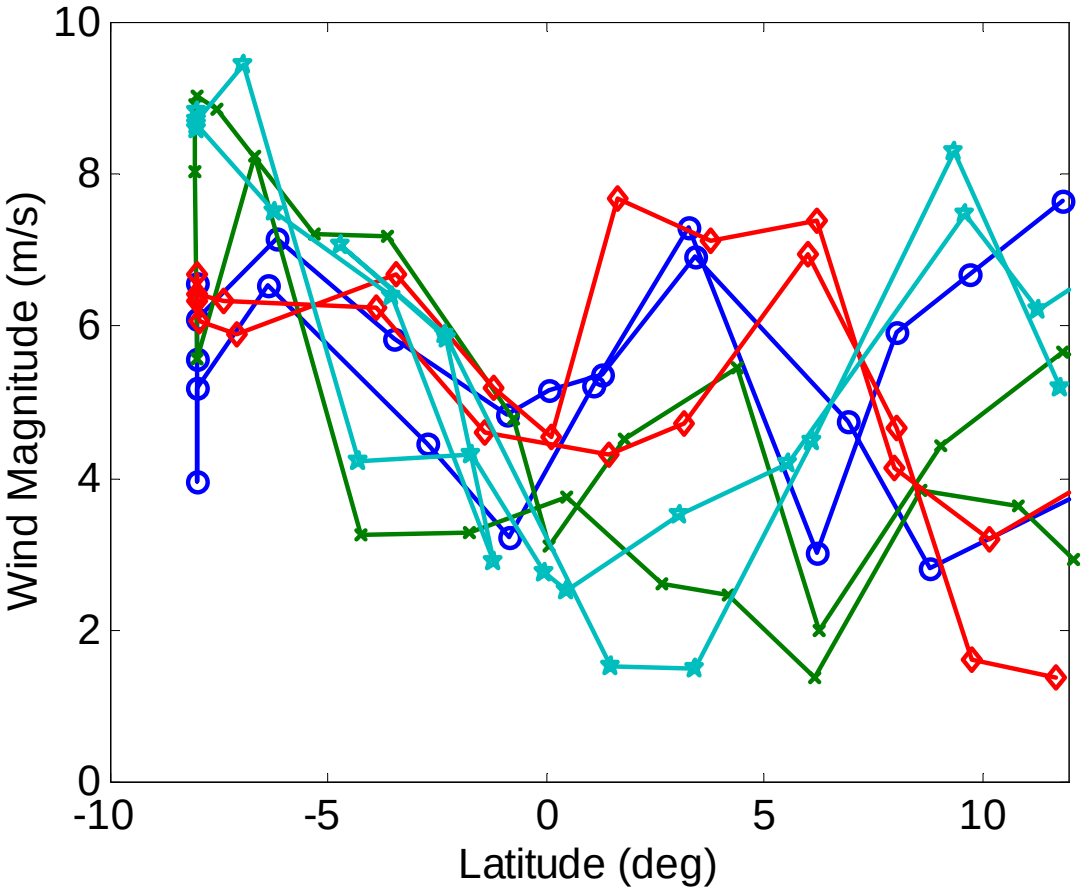

Figure 4a. Wind speed versus latitude (daily average values) for the four missions (Fall99 - Spring 01). Symbols are as follows: circle - fall99; x - spring00; diamond - fall00; star - spring01.

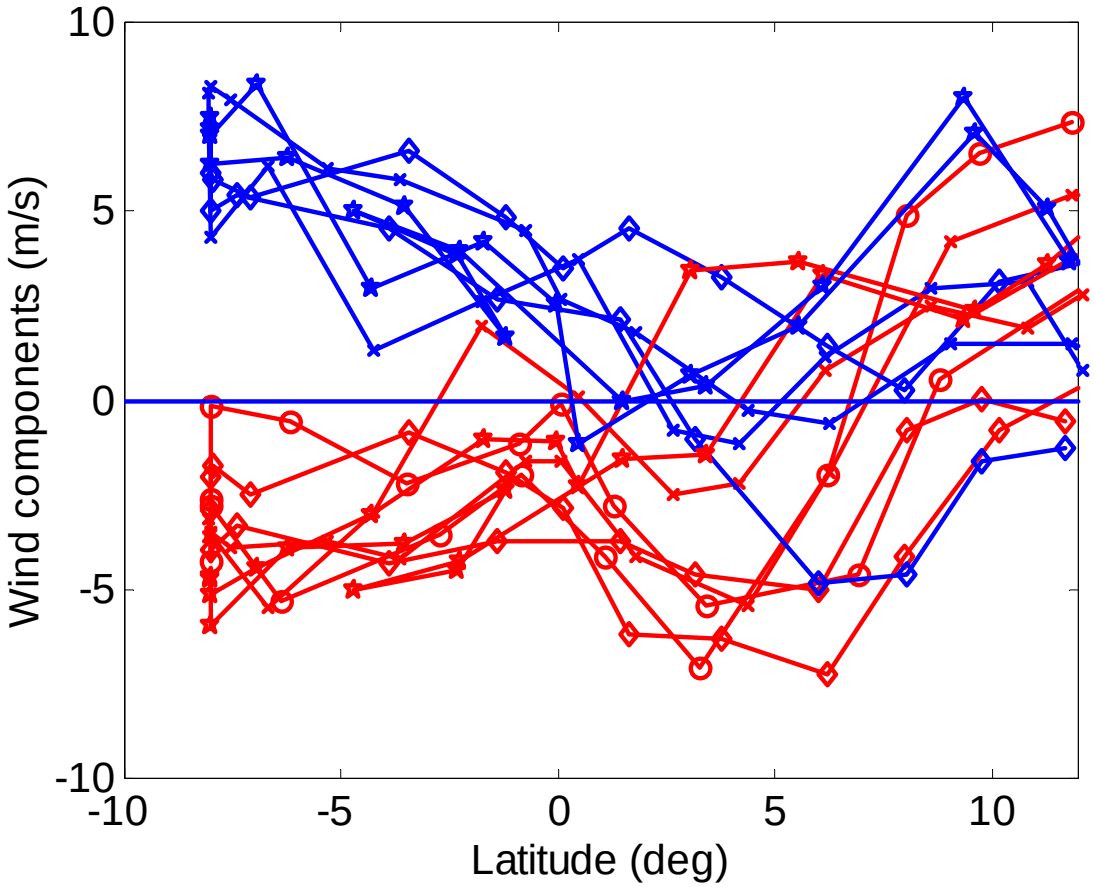

Figure 4b. Wind components (red - from the north; blue - from the east) versus latitude (daily average values) for the four missions (Fall99 - Spring 01). Symbols are as follows: circle - fall99; x - spring00; diamond - fall00; star - spring01.

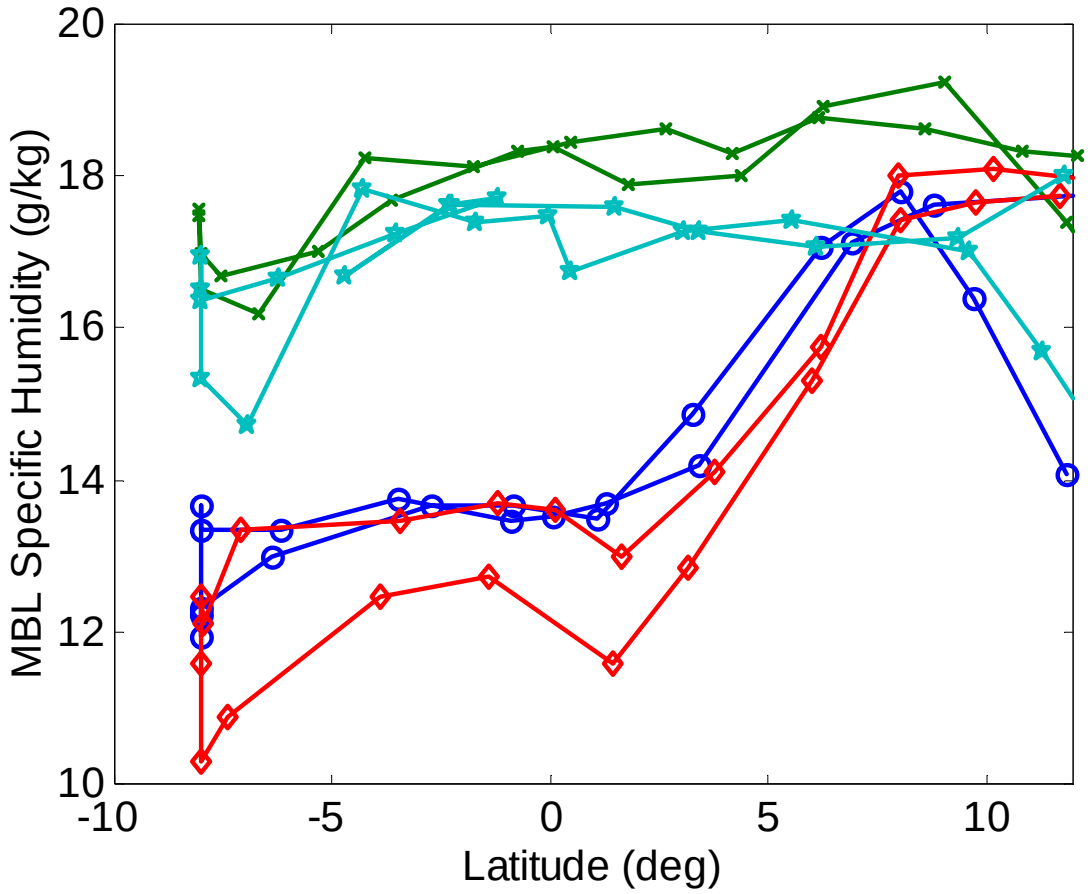

Figure 5a. Specific humidity (15-m) versus latitude (daily average values) for the four missions (Fall99 - Spring 01). Symbols are as follows: circle - fall99; x - spring00; diamond - fall00; star - spring01.

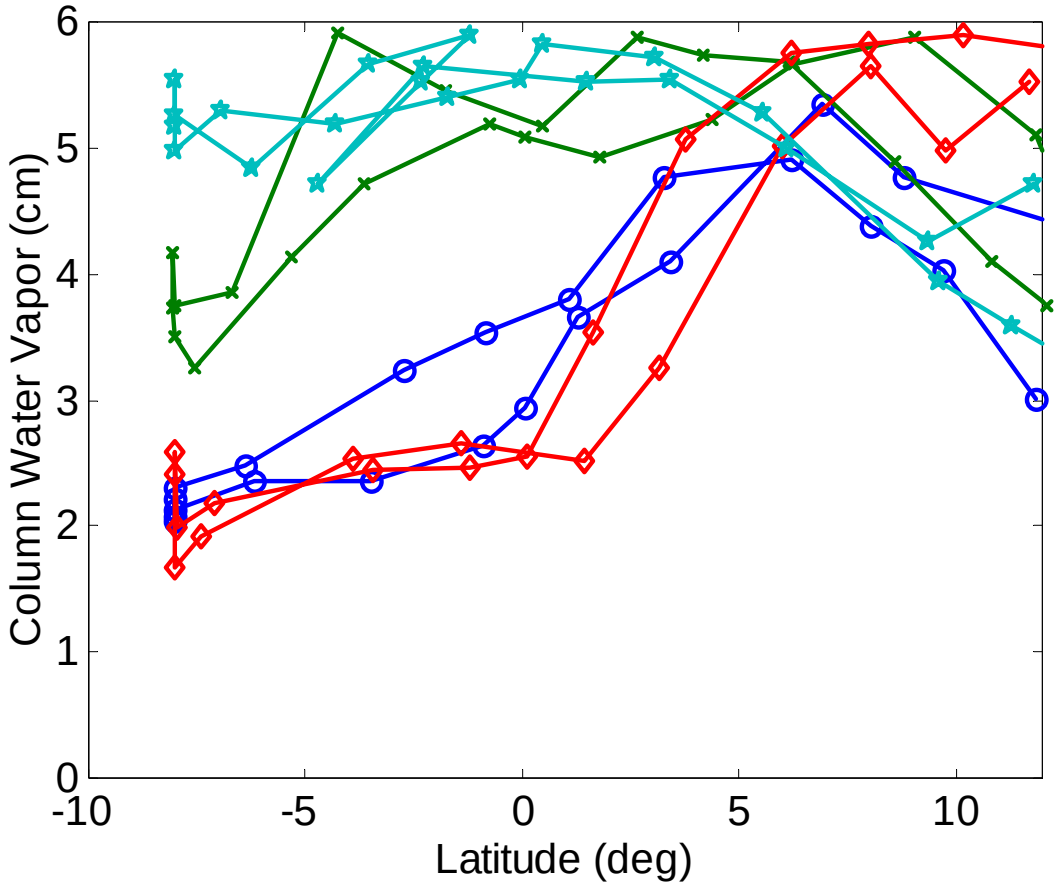

Figure 5b. Column-integrated total water vapor (precipitable water) from the MWR versus latitude (daily average values) for the four missions (Fall99 - Spring 01). Symbols are as follows: circle - fall99; x - spring00; diamond - fall00; star - spring01.

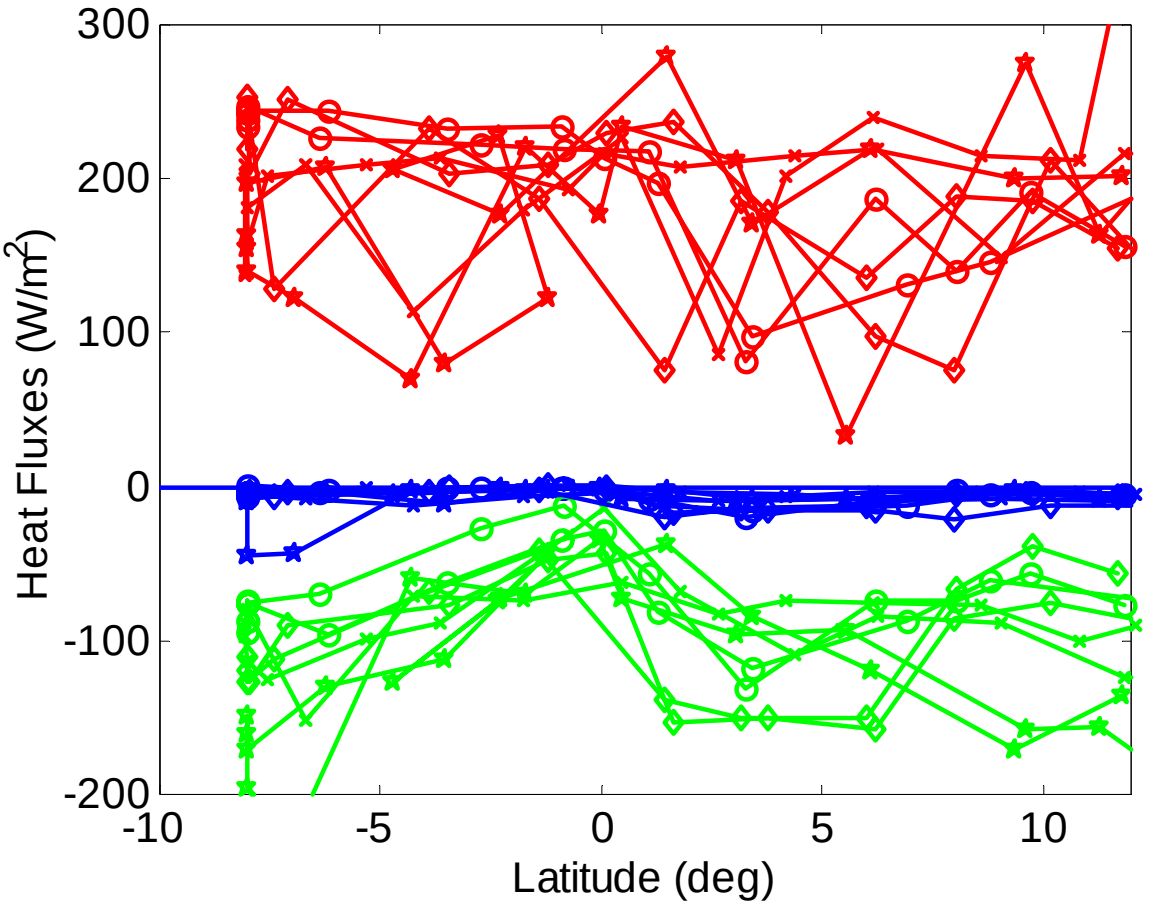

Figure 6. The three primary surface heat flux components (blue - sensible, red - net radiation, and green - latent) versus latitude (daily average values) for the four missions (Fall99 - Spring 01). Symbols are as follows: circle - fall99; x - spring00; diamond - fall00; star - spring01.

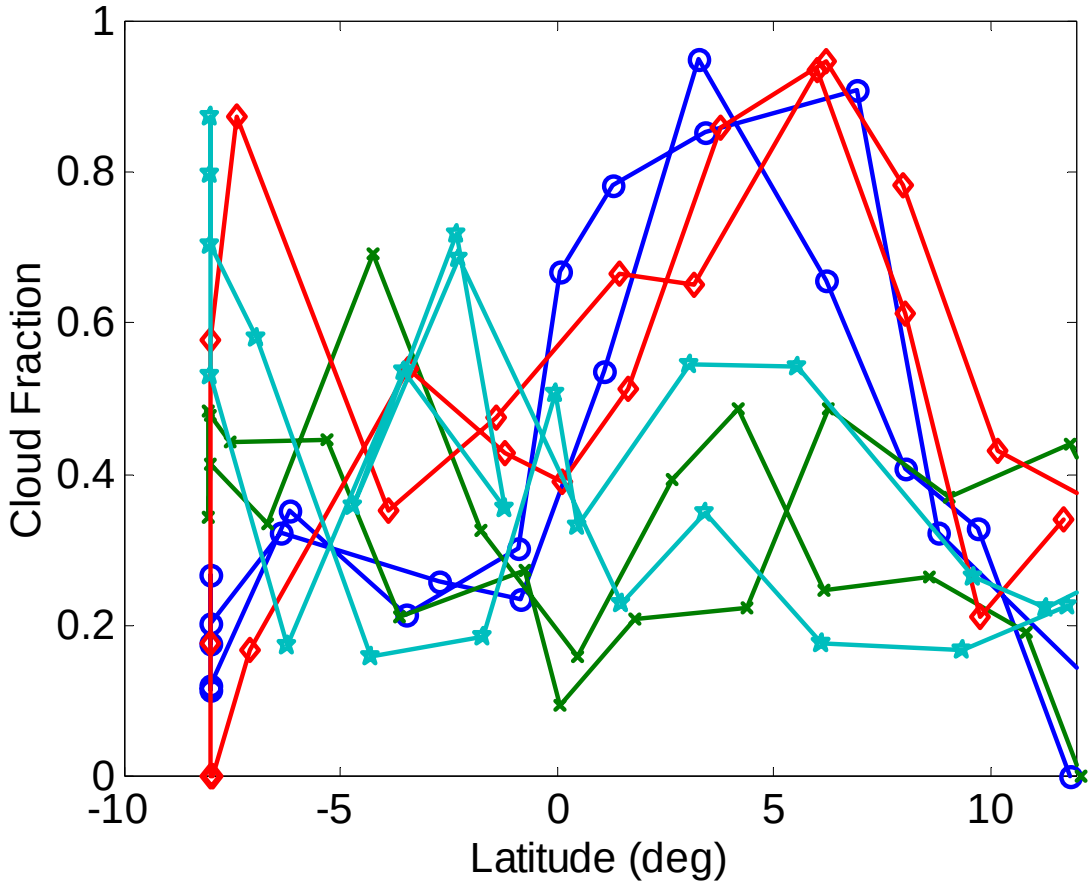

Figure 7. Vertical cloud fraction versus latitude (daily average values) for the four missions (Fall99 - Spring 01). Symbols are as follows: circle - fall99; x - spring00; diamond - fall00; star - spring01.

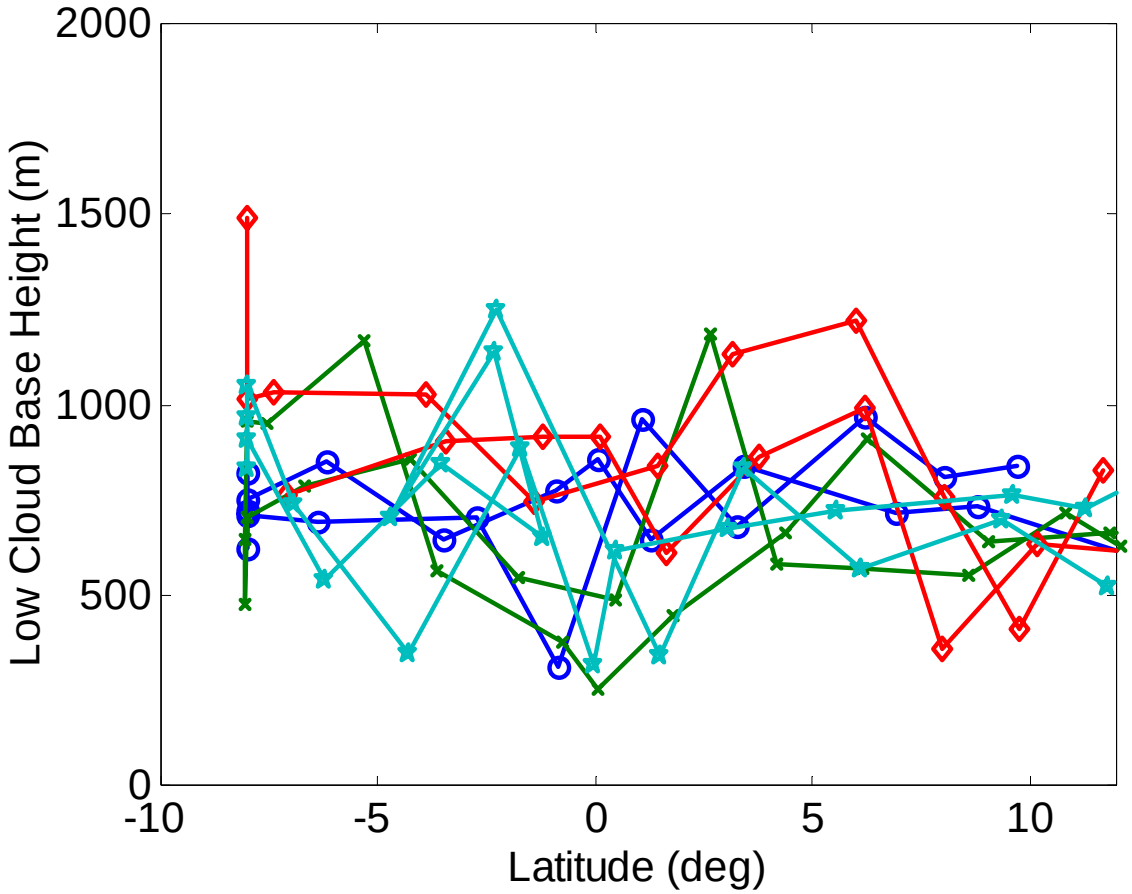

Figure 8. Lowest 15% cloud base height (hourly distribution) versus latitude (daily average values) for the four missions (Fall99 - Spring 01). Symbols are as follows: circle - fall99; x - spring00; diamond - fall00; star - spring01.

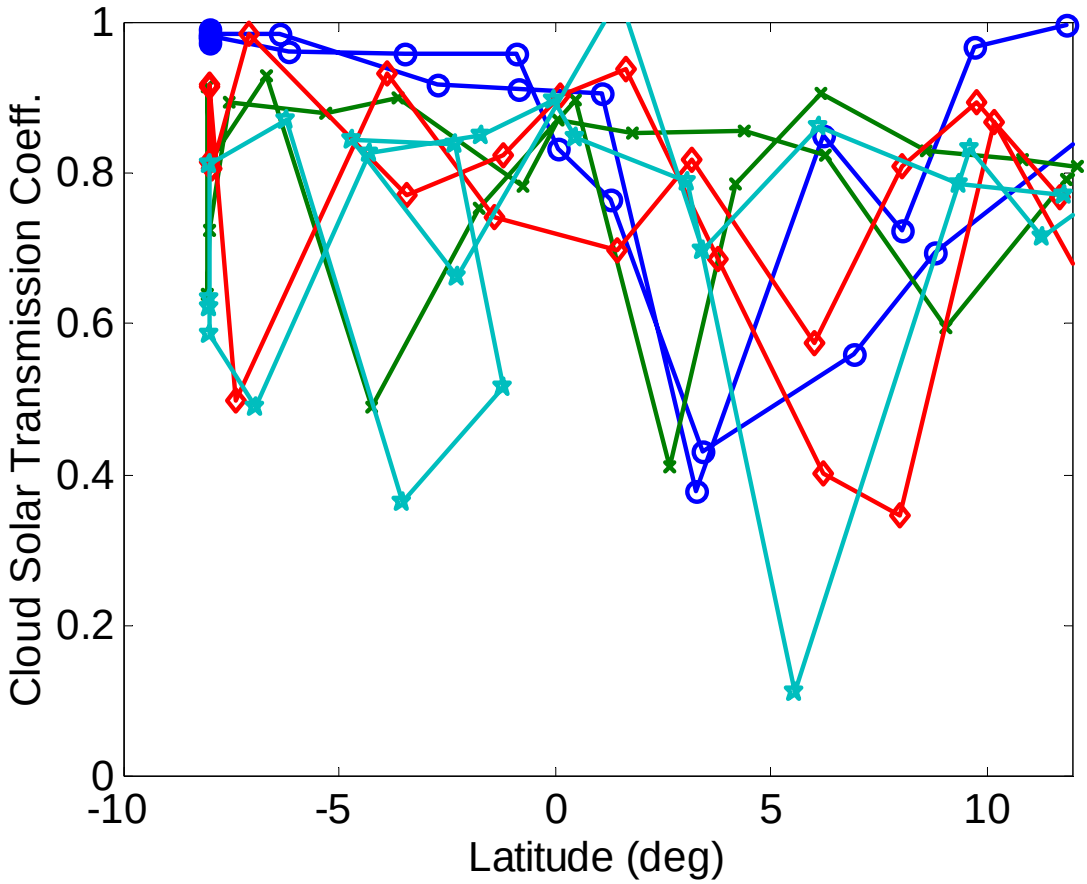

Figure 9. Cloud solar radiative flux transmission coefficient versus latitude (daily average values) for the four missions (Fall99 - Spring 01). This is the daily mean measured solar flux divided by the daily mean computed clear sky flux. Symbols are as follows: circle - fall99; x - spring00; diamond - fall00; star - spring01.

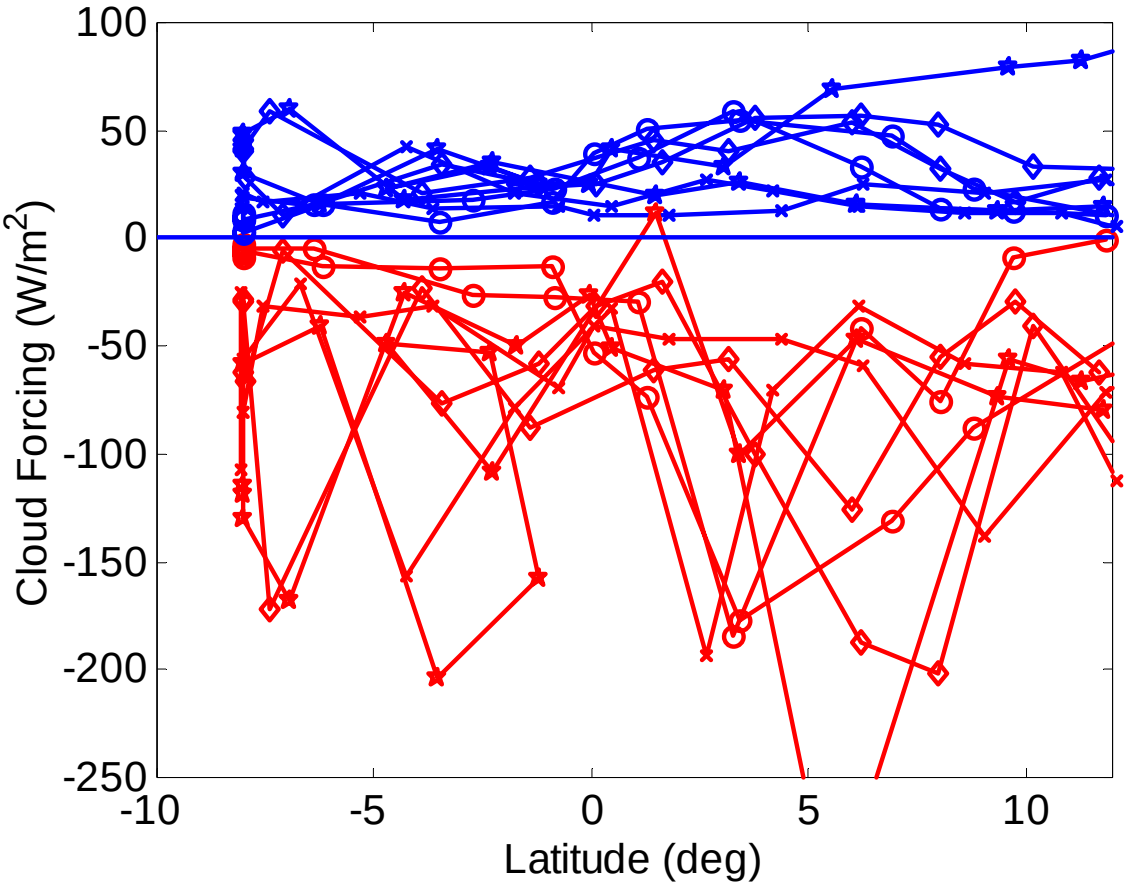

Figure 10. Surface cloud forcing (blue - IR, red - solar) versus latitude (daily average values) for the four missions (Fall99 - Spring 01). Symbols are as follows: circle - fall99; x - spring00; diamond - fall00; star - spring01.

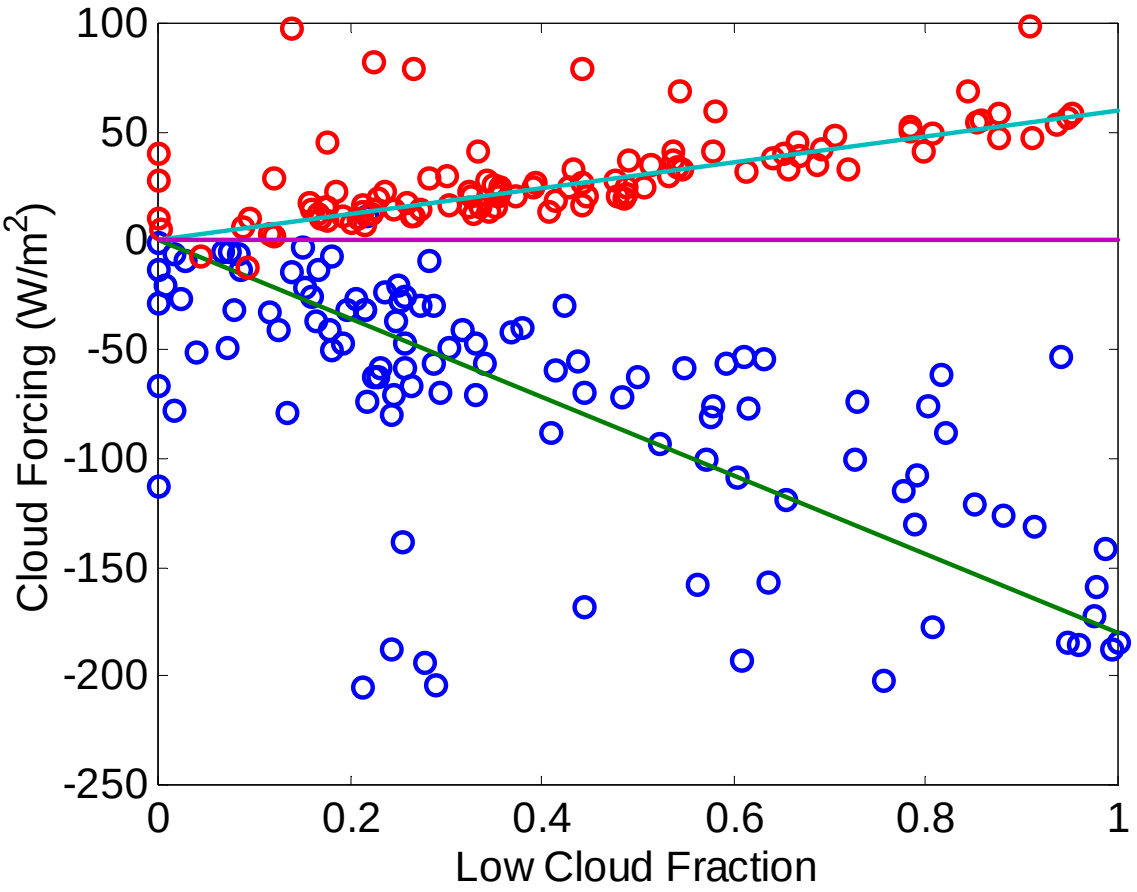

Figure 11. Surface cloud forcing (blue - IR, red - solar) versus cloud fraction (daily average values) for the four missions (Fall99 - Spring 01). Symbols are as follows: circle - fall99; x - spring00; diamond - fall00; star - spring01. The solid lines follow from (2) with MLCF = + 60 W/m^2 and MSCF = -180 W/m^2.

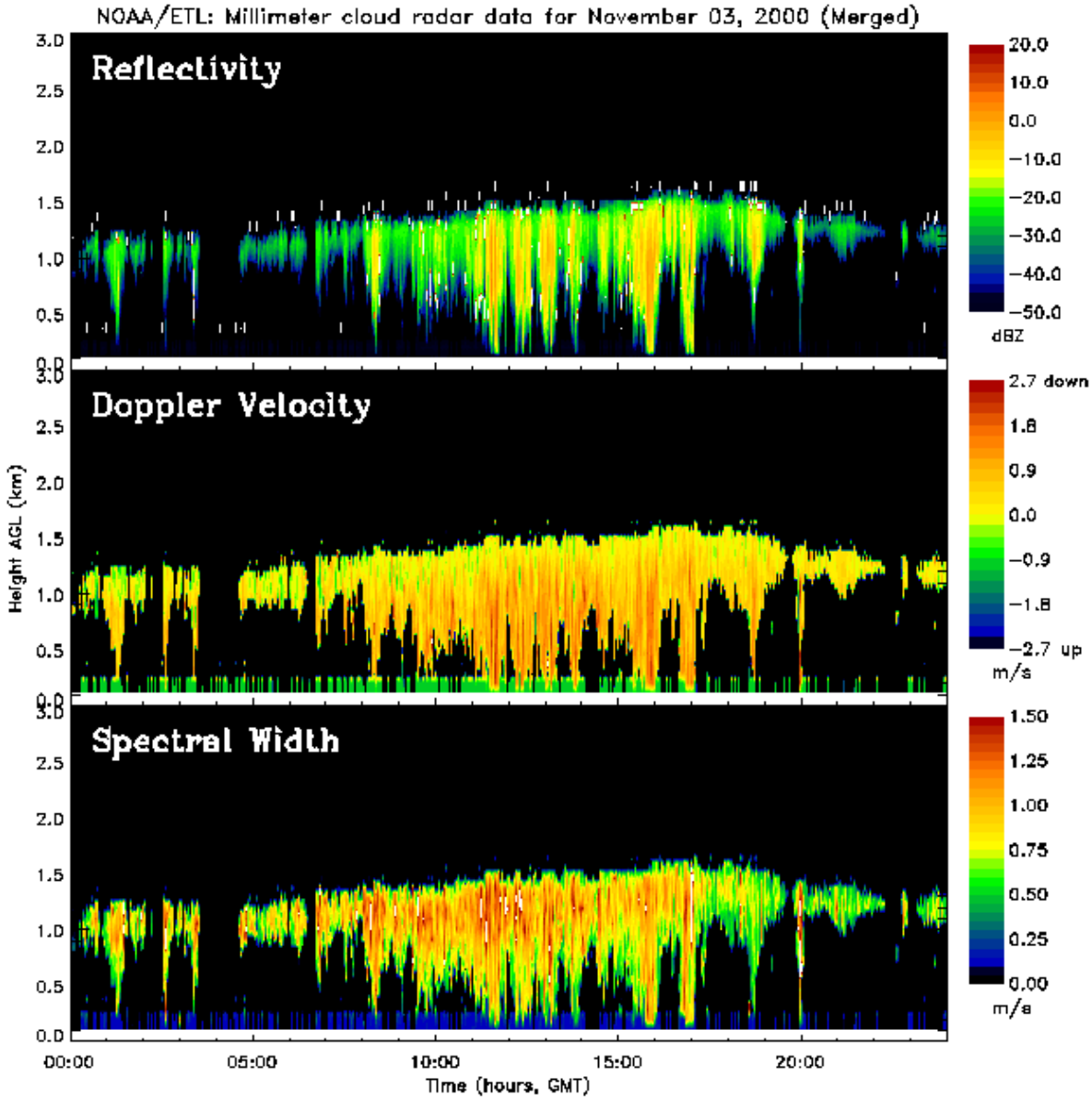

Figure 12a. Time-height cross section of 35 GHz radar backscatter (upper panel), mean Doppler shift (middle panel) and Doppler width (bottom panel) for November 3, 2000. These data were taken at about 8 S 95 W.

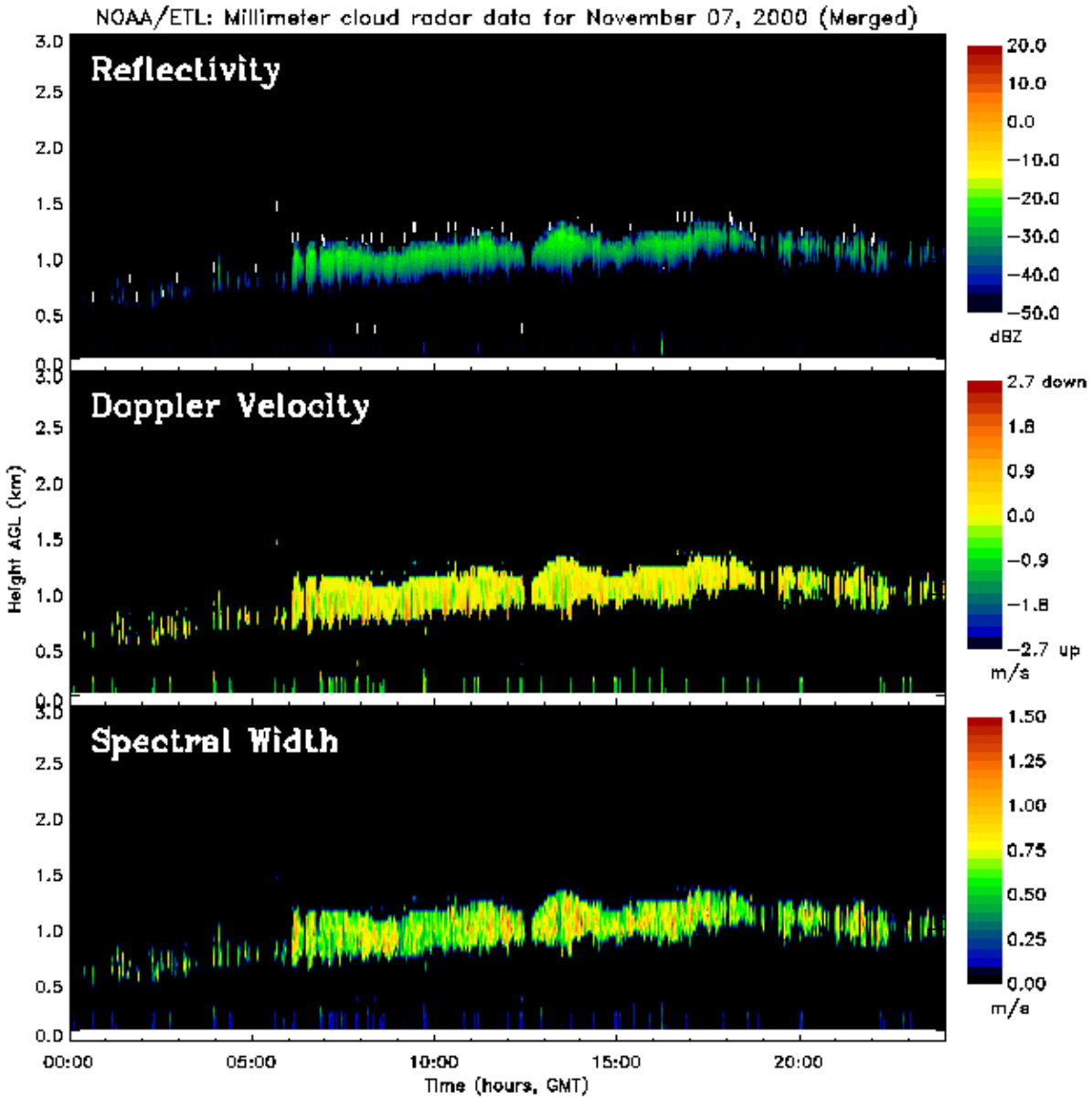

Figure 12b. Time-height cross section of 35 GHz radar backscatter (upper panel), mean Doppler shift (middle panel) and Doppler width (bottom panel) for November 7, 2000. These data were taken at about 0 N 95 W.